

Tuneable paramagnetic susceptibility and exciton g-factor in Mn-doped PbS colloidal nanocrystals

Supplementary information

S1. Raman Spectroscopy

For Raman measurements samples were drop-casted on glass or quartz slides. Raman spectra were acquired at $T = 300\text{K}$ using laser excitation at $\lambda = 633\text{nm}$ and power density $P = 100\text{W}/\text{cm}^2$. Figure S1a shows the Raman spectra of undoped and Mn-doped PbS QDs. For PbS QDs, the spectrum reveals a peak at 203 cm^{-1} corresponding to the PbS longitudinal optical (LO) phonon (LO peak of bulk PbS is at 206 cm^{-1}) [1]. The incorporation of Mn into the nanoparticles induces a systematic linear shift of the LO peak (Figure S1a-b), which we attribute to the Mn-induced change in the composition of the nanocrystals.

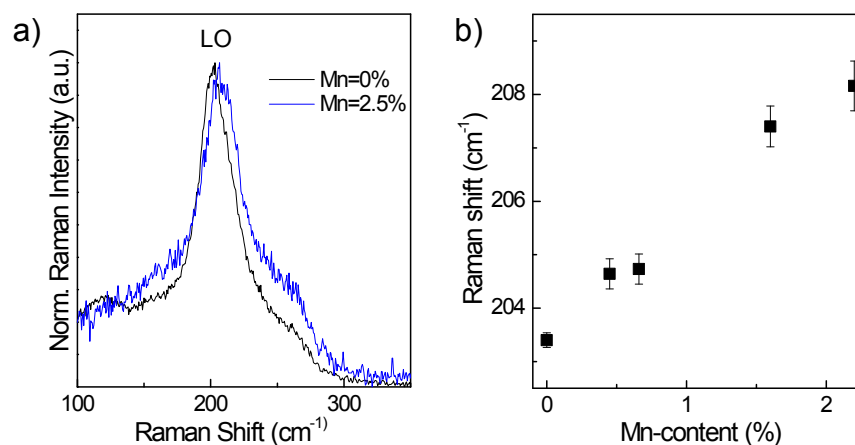


Figure S1 (a) Room temperature Raman spectra for PbS and Mn-doped PbS (Mn = 2.5 %) nanocrystals. **(b)** Raman shift of the LO-phonon Raman peak with increasing Mn-content.

[1] A. V. Baranov, K. V. Bogdanov, E. V. Ushakova, A. V. Cherevko, A. V. Fedorov, and S. Tschardtke, *Optics and Spectroscopy* **2010**, 109, 268.

S2. Magnetic susceptibility measurements

In our experiment a cylindrical plastic sample container with volume of 1 ml was suspended inside the magnet bore by a glass fiber (Figure S2). The fiber was hung from an electronic balance in order to measure the vertical force on the sample, which is the sum of its weight and the magnetic force acting on it. The magnet bore was filled with dry N₂ gas at atmospheric pressure to displace the oxygen in the air, which, being paramagnetic, gives rise to undesirable thermomagnetic convection within the bore and can contaminate the liquid sample. The sample container was filled with de-gassed pure water and suspended in the upper section of the bore. Here, the water, being diamagnetic, was repelled upwards away from the strong magnetic field at the center of the solenoid coils by a magnetic force $F = \chi VG$ where $\chi = -9 \times 10^{-6}$ is the magnetic volume susceptibility of water, V is the volume, $G = (1/\mu_0)B \partial B/\partial z$, B is the magnitude of the magnetic field and $\partial B/\partial z$ is its vertical gradient. We use the convention that positive (negative) F indicates an upward (downward) force. Since G is a negative quantity in this position, F is positive, indicating an upward force.

The balance measures the vector sum of the magnetic and gravitational forces acting on the sample container and its contents, the fiber and the brass weight. The vertical position of the sample was adjusted by a screw with fine pitch until it hung where the vertical force on the sample was a minimum; at this point, $|G|$ is a maximum. The electric current in the solenoid was then varied until the force on a water-filled container was equal to the force on an 'empty' container (*i.e.* container filled only with N₂ gas at atmospheric pressure).

This procedure gives us an accurate measure of G within the sample container, in terms of the magnetic susceptibility of water: under these conditions the mean value of G within the sample is $G_0 = \rho g/\chi$, where $\rho = 1 \text{ g/cm}^3$ is the density of water and $g = 9.8 \text{ ms}^{-2}$. The force F_{QD} on a sample consisting of a suspension of colloidal QDs in water was then measured. The difference in force measured by the balance, $\Delta F = F_{QD} - F_{water}$, is due only to the magnetic force on the QDs (note that ΔF is negative if there is a greater downward force on the sample containing the QDs than on the water-only sample).

The magnetic mass susceptibility of the QDs is given by

$$\chi_m = \frac{1}{G_0} \left(\frac{F_{QD}}{m_{QD}} + g \right), \quad (1)$$

where m_{QD} is the total mass of QDs in the sample. In this case the weight is small compared to the difference in magnetic force ΔF so that we have $\chi_m \approx \Delta F/G_0 m_{QD}$ to a good approximation.

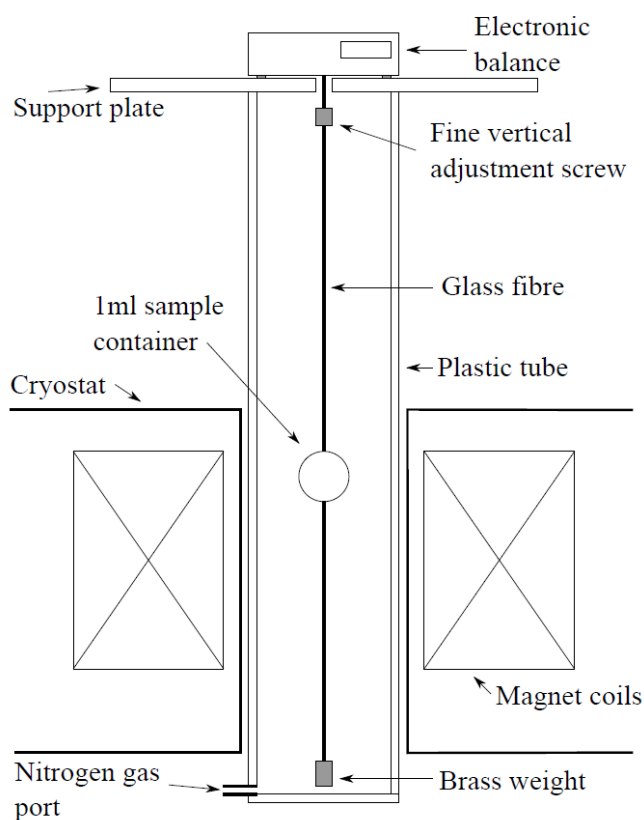


Figure S2 Schematic diagram of the experimental set-up used for magnetic susceptibility measurements.

S3. PL lifetime measurements

The PL lifetime measurements were performed on QD samples drop-casted onto a quartz substrate. The excitation was provided by the 532nm line of a Nd:YAG laser (~ 8 ns pulse) using short- and long-pass interference filters to remove other harmonics. The PL was collected and focused onto the slits of a monochromator using long-pass interference filter (FEL700, Thorlabs). The monochromator grating was a 600 g/mm blazed at $1\mu\text{m}$. The PL was detected with a liquid N_2 -cooled NIR- photomultiplier tube (C5594, Hamamatsu) and the transient decay was recorded using 1GHz oscilloscope (Agilent Infinium). The system response time was measured to be 20 ns.

The PL decay curves (Figure S3) are fitted using a biexponential function. We find that PbS QDs have lifetimes $\tau_1 = 0.6 \mu\text{s}$ and $\tau_2 = 2.5 \mu\text{s}$ at $T = 4\text{K}$, and $\tau_1 = 0.2 \mu\text{s}$ and $\tau_2 = 1.3\mu\text{s}$ at $T = 250\text{K}$. The measured values are similar to those reported previously for PbS QDs [1-2]. The incorporation of Mn tends to reduce the lifetime: for Mn = 5%, τ is reduced by a factor of ~ 3 at each temperature.

The origin of the biexponential nature of the PL decay PbS QDs remains unresolved. Similar behavior was reported for II-VI QDs with a number of alternative explanations including emission from surface trap states [3], deep trap states in QD solids [4], and dark-exciton states [1-2, 5] have been invoked. Many of these studies utilize a 3-level system to fit the temperature dependence of measured optical properties giving predicted values of the singlet-triplet exciton energy splitting, ΔE [1-2, 5]. In our studies the observation of biexponential decay at $T = 5\text{K}$ could be indicative of either a small value of ΔE , the creation of a Mn-associated emitting trap states, or splitting of the lower energy (triplet) level, *e.g.* via the exchange interaction coupling of Mn-ion spins, to create two emitting states with different lifetimes. The creation of Mn-related trap states, whilst potentially leading to a reduction in radiative lifetime with doping, would not be expected to lead to the large blueshift in the PL spectra observed (Figure 1a) with increasing doping concentration. To explain this modification of the nanocrystal, confinement potential is required for example as predicted using Vegard's law for alloys. As such, modification of the singlet-triplet exchange splitting and state mixing by the incorporation of Mn remains a most likely scenario with a further effect on spin-relaxation time in these QDs. This would be in agreement with the observed dependence of the radiative lifetime and τ_s/τ on Mn-concentration.

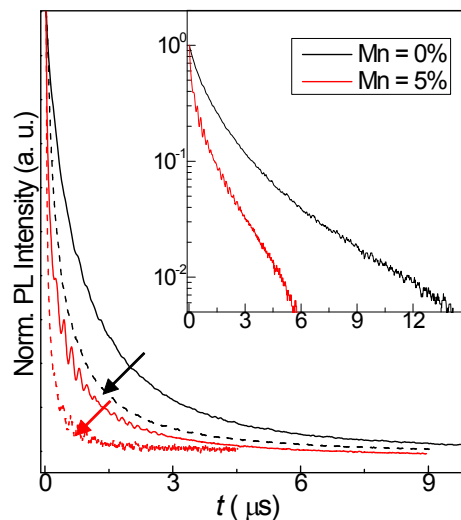


Figure S3 PL decay curves for PbS (black lines) and Mn-doped PbS QDs with 5% Mn measured at $T = 5\text{K}$ (continuous line) and at $T = 250\text{K}$ (dashed line). Inset shows a logarithmic plot of the transient decays at $T = 5\text{K}$.

[1] Nordin M. N.; Li J.; Clowes S. K.; Curry R. J. Temperature Dependent Optical Properties of PbS Nanocrystals. *Nanotechnology* **2012**, 23, 275701.

[2] Wang J.; Mandelis A.; Melnikov A.; Hoogland S.; Sargent E. H. Exciton Lifetime Broadening and Distribution Profiles of PbS Colloidal Quantum Dot Thin Films Using Frequency- and Temperature-Scanned Photocarrier Radiometry. *J. Phys. Chem. C* **2013**, 117, 23333.

[3] J. Gao and J. C. Johnson, Charge Trapping in Bright and Dark States of Coupled PbS Quantum Dot Films. *ACS Nano* **2012**, 6, 3292.

[4] Bozyigit D.; Volk S.; Yarema O.; Wood V. Quantification of Deep Traps in Nanocrystal Solids, Their Electronic Properties, and Their Influence on Device Behavior. *Nano Lett.* **2013**, 13, 5284.

[5] Yue F.; Tomm J. W.; Kruschke D. Spontaneous and Stimulated Emission Dynamics of PbS Quantum Dots in a Glass Matrix. *Phys. Rev. B* **2013**, 87, 195314.